Determination of the in Vivo Stoichiometry of Tyrosyl Radical per $\beta\beta'$ in *Saccharomyces cerevisiae* Ribonucleotide Reductase†

Allison D. Ortigosa,‡,§ Daniela Hristova,‡,§ Deborah L. Perlstein,‡,§,|| Zhen Zhang,⊥ Mingxia Huang,⊥ and JoAnne Stubbe*,‡

Departments of Chemistry and Biology, Massachusetts Institute of Technology, Cambridge, Massachusetts 02139, and Department of Biochemistry and Molecular Genetics, University of Colorado Health Sciences Center, Aurora, Colorado 80045

Received May 25, 2006; Revised Manuscript Received July 31, 2006

ABSTRACT: The class I ribonucleotide reductases catalyze the conversion of nucleotides to deoxynucleotides and are composed of two subunits: R1 and R2. R1 contains the site for nucleotide reduction and the sites that control substrate specificity and the rate of reduction. R2 houses the essential diferric-tyrosyl radical ($Y^{\bullet}$) cofactor. In *Saccharomyces cerevisiae*, two R1s, α_n and α'_n, have been identified, while R2 is a heterodimer ($\beta\beta'$). β' cannot bind iron and generate the $Y^{\bullet}$; consequently, the maximum amount of $Y^{\bullet}$ per $\beta\beta'$ is 1. To determine the cofactor stoichiometry in vivo, a FLAG-tagged β ($^{FLAG}\beta$) was constructed and integrated into the genome of Y300 (MHY343). This strain facilitated the rapid isolation of endogenous levels of $^{FLAG}\beta\beta'$ by immunoaffinity chromatography, which was found to have 0.45 ± 0.08 $Y^{\bullet}/^{FLAG}\beta\beta'$ and a specific activity of 2.3 ± 0.5 μmol min^{-1} mg^{-1}. $^{FLAG}\beta\beta'$ isolated from MMS-treated MHY343 cells or cells containing a deletion of the transcriptional repressor gene *CRT1* also gave a $Y^{\bullet}/^{FLAG}\beta\beta'$ ratio of 0.5. To determine the $Y^{\bullet}/\beta\beta'$ ratio without R2 isolation, whole cell EPR and quantitative Western blots of β were performed using different strains and growth conditions. The wild-type (wt) strains gave a $Y^{\bullet}/\beta\beta'$ ratio of 0.83−0.89. The same strains either treated with MMS or containing a *crt1*Δ gave ratios between 0.49 and 0.72. Nucleotide reduction assays and quantitative Western blots from the same strains provided an independent measure and confirmation of the $Y^{\bullet}/\beta\beta'$ ratios. Thus, under normal growth conditions, the cell assembles stoichiometric amounts of $Y^{\bullet}$ and modulation of $Y^{\bullet}$ concentration is not involved in the regulation of RNR activity.

Ribonucleotide reductase (RNR)[1] catalyzes the reduction of ribonucleotides to deoxyribonucleotides, providing the monomeric building blocks required for DNA replication and DNA repair (*1*−*3*). The class I RNRs, present in eubacteria, eukaryotes, bacteriophages, and viruses, are composed of two subunits: R1 and R2. The quaternary structure of R1 in *Escherichia coli* is believed to be α_2 and in mouse can be α_2, α_4, and α_6 (*4*−*7*). R1 contains the active site where the radical-based chemistry of nucleotide reduction occurs and the allosteric effector binding sites that control both the specificity of nucleotide reduction and enzymatic activity. The quaternary structure of R2 is a homodimer (β_2) and contains the diferric-tyrosyl radical ($Y^{\bullet}$) cofactor essential for RNR activity. The active form of RNR is a complex of R1 and R2.

Since the seminal identification of Y122 as the amino acid residue harboring the $Y^{\bullet}$ in *E. coli* R2, numerous R2s from a diverse range of organisms have been cloned and overproduced in heterologous expression systems (*3*, *8*, *9*). R2 is usually isolated in an apo state or in a state in which the cofactor is substoichiometrically assembled, 0.2−1.5 $Y^{\bullet}$ per R2 (*10*−*16*). Chelation of iron from R2 followed by reconstitution with Fe^{2+}, O_2, and a reductant usually leads to an increase in the amount of diferric-$Y^{\bullet}$ cofactor (*17*). However, stoichiometric amounts of $Y^{\bullet}$ (one $Y^{\bullet}$ per β) have never been observed in vivo or in vitro for any system. Whether R2 contains one or two tyrosyl radicals per R2 in vivo, with the former requiring an asymmetric R1−R2 complex that could have important mechanistic implications, remains an open question.

Our inability to assemble stoichiometric amounts of cofactor in vitro and in heterologous expression systems suggests that in vivo, cluster assembly requires unidentified protein(s) or small molecule components. The activity of *E. coli* RNR in vitro has been shown to directly correlate with

† A.D.O. was supported in part by NIH Training Grant 5T32 CA 09112-28 and Anna Fuller Fellowship 2300500. D.L.P. was supported by NIH Training Grant 5T32 CA 09112-20. J.S. acknowledges support of NIH Grant GM29595. M.H. acknowledges support of NIH Grant CA095207 and ACS Grant RSG0305001.

* To whom correspondence should be addressed. Telephone: (617) 253-1814. Fax: (617) 258-7247. E-mail: stubbe@mit.edu.

‡ Massachusetts Institute of Technology.

§ These authors contributed equally to this work.

|| Present address: Department of Microbiology and Molecular Genetics, Harvard Medical School, Boston, MA 02115.

⊥ University of Colorado Health Sciences Center.

[1] Abbreviations: Abs, antibodies; AEBSF, 4-(2-aminoethyl)benzenesulfonyl fluoride; α, polypeptide encoded by *RNR1*; α′, polypeptide encoded by *RNR3*; β, polypeptide encoded by *RNR2*; β′, polypeptide encoded by *RNR4*; HU, hydroxyurea; E-64, (2*S*,3*S*)-3-(*N*-{(*S*)-1-[*N*-(4-guanidinobutyl)carbamoyl]-3-methylbutyl}carbamoyl)oxirane-2-carboxylic acid; MMS, methylmethane sulfonate; PBS, phosphate-buffered saline; R1(α_n,α'_n), ribonucleotide reductase large subunit; R2($\beta\beta'$), ribonucleotide reductase small subunit; *RNR1* and *RNR3*, genes encoding *S. cerevisiae* RNR large subunit; *RNR2* and *RNR4*, genes encoding the *S. cerevisiae* RNR small subunit; RNR, ribonucleotide reductase; wt, wild type; $Y^{\bullet}$, tyrosyl radical.

10.1021/bi0610404 CCC: $33.50
Published on Web 09/13/2006

Table 1: Yeast Strains Used in This Study

strain	genotype	ref
BY4741 (S288C background)	MATa, his3Δ1, leu2Δ0, met15Δ0, ura3Δ0	*35*
BY4741-*crt1*Δ (S288C background)	BY4741 rfx1::KAN	*35*
Y300 (W303 background)	MATa, trp1-1, ura3-1, his3-11,15, leu2-3,112, ade2-1, can1-100	this study
MHY619 (W303 background)	MATa, his3, ura3, rnr2::FLAG-RNR2-Kan, crt1::LEU2	this study
MHY343 (W303 background)	MATx, can1-100, ade2-1, his3-11,14, leu2-3, trp1-1, ura3-1, rnr2::FLAG-RNR2-Kan	*14*
PS0799 (W303 background)	MATa, ade2-1, trp1-1, can1-100, leu2-3,112, his3-11, ura3	*28*

the concentration of Y$^\bullet$ and is proposed to directly correlate in other organisms as well (*18*). However, the in vivo amount of Y$^\bullet$ per R2 has never been determined in any organism. Regulation of the levels of Y$^\bullet$ could provide an additional mechanism for controlling deoxynucleotide pools during DNA replication and repair (*19*−*21*). In this paper, we present the first measurements of the ratio of Y$^\bullet$ per R2 in a number of strains of *Saccharomyces cerevisiae* grown in the absence or presence of the DNA-damaging agent methylmethane sulfonate (MMS).

S. cerevisiae has four genes encoding RNR subunits: *RNR1*, *RNR2*, *RNR3*, and *RNR4*. *RNR1* and *RNR3* encode the R1 subunits. The proteins are designated α and α′ and are both monomers in the absence of allosteric effectors (*22*−*24*). At present, the active oligomeric state(s) of α_n (α_2, α_4, and α_6) has not been established. *RNR2* and *RNR4* encode the R2 subunits: β_2 and β'_2 (*25*−*27*). Recent biochemical and genetic studies have established that in *S. cerevisiae* the active form of R2 is the $\beta\beta'$ heterodimer (*14*, *15*, *28*−*30*). Three of the six amino acids involved in iron binding in β' are mutated relative to β and other R2s in general (*26*, *27*). In addition, a Tyr-to-Phe substitution at the Tyr designed to be oxidized has no effect on β' function in vivo (*27*). Thus, $\beta\beta'$ can maximally contain a single diferric-Y$^\bullet$ cofactor located in the active site of β. To date, two strategies for isolating $\beta\beta'$ have been reported: one in which β and β' are separately expressed in *E. coli*, isolated, mixed in a 1:1 ratio and the cofactor reconstituted and a second in which β and β' are coexpressed in *E. coli* and the cofactor assembled during growth (*15*, *28*). Both strategies give substoichiometric amounts of Y$^\bullet$ (0.2−0.4 Y$^\bullet$/$\beta\beta'$).

To determine the in vivo radical stoichiometry (Y$^\bullet$/$\beta\beta'$ ratio) in *S. cerevisiae*, three approaches have been taken. In the first approach, an N-terminally FLAG-tagged *RNR2* was generated and integrated into the genome in place of *RNR2* in the Y300 strain (MHY343) and a *crt1*Δ Y300 strain (MHY619). Crt1 (also known as Rfx1) is a repressor of transcription of *RNR2*, *RNR3*, and *RNR4* (*31*−*33*). Transcriptional repression is relieved in response to checkpoint activation by DNA damage or replication blocks. Thus, the levels of $\beta\beta'$ (and α′) are significantly elevated in the *crt1*Δ strain relative to the wt strain. The FLAG tag allowed rapid isolation of endogenously expressed $^{FLAG}\beta$ from crude extracts of both MHY343 and MHY619 cells. The amount of diferric-Y$^\bullet$ cofactor as well as the specific activity of $^{FLAG}\beta\beta'$ was determined. In the second approach, the Y$^\bullet$/$\beta\beta'$ or Y$^\bullet$/$^{FLAG}\beta\beta'$ ratios were determined by whole cell EPR spectroscopy and quantitative Western blotting of crude extracts from three wt strains grown in the presence and absence of MMS (BY4741, Y300, and PS0779) and two *crt1*Δ strains (BY4741-*crt1*Δ and MHY619) (see Table 1). In the third approach, steady-state kinetic assays and quantitative Western blots were performed to measure the specific activities of β and $^{FLAG}\beta$ from partially purified crude extracts from the same aforementioned strains. The concentration of the Y$^\bullet$ is shown to directly correlate with RNR activity, thus providing an alternative way to measure the amount of Y$^\bullet$/$\beta\beta'$ or Y$^\bullet$/$^{FLAG}\beta\beta'$. These studies show that in vivo with different wt *S. cerevisiae* strains, R2 contains 0.83−0.89 Y$^\bullet$/$\beta\beta'$. In the cases in which these wt strains are insulted with a DNA-damaging agent or contain a *crt1*Δ, the level of β expression is increased 4−30-fold relative to that of wt and the Y$^\bullet$/$\beta\beta'$ ratios vary from 0.49 to 0.72.

MATERIALS AND METHODS

[U-^{14}C-*cytosine*]CDP (50 mCi/mmol) was obtained from Moravek Biochemical (Brea, CA). Poly(vinylidene) difluoride (PVDF, Immun-Blot) membranes, the Silver Stain Plus Kit, and Criterion 10% Tris-HCl SDS−PAGE gels were obtained from Bio-Rad. Secondary antibodies (Abs, horseradish peroxidase-conjugated donkey anti-rabbit Abs), Complete protease inhibitor tablets, calf intestinal alkaline phosphatase, and DNase I from bovine pancreas were obtained from Roche. $^{His}\beta_2$ and β'_2 were isolated from an *E. coli* expression system, and the heterodimer was reconstituted as described previously (*28*). $^{His}\beta\beta'$ typically contained 0.1−0.2 Y$^\bullet$ and had a specific activity of 1.5−1.8 μmol min^{-1} mg^{-1}. α was isolated from an *E. coli* expression system as previously described and has a specific activity of ∼200 nmol min^{-1} mg^{-1} using $^{His}\beta\beta'$ containing 0.1−0.2 Y$^\bullet$ (*30*). The concentration of α was determined by Bradford assay with BSA as a standard and is reported as a monomer. Anti-FLAG agarose, 3×-FLAG peptide (three tandem copies of the FLAG epitope), Bradford reagent, and all other reagents and chemicals were obtained from Sigma-Aldrich. The concentrations of $^{His}\beta\beta'$ and $^{FLAG}\beta\beta'$ were determined using an $\epsilon_{280-310}$ of 99 800 M^{-1} cm^{-1} and is reported as a concentration of monomer β or dimer $\beta\beta'$ (*28*). Iron concentrations were determined by the ferrozine assay (*34*).

Yeast Strain Construction. The yeast strains used in this study are listed in Table 1. Yeast strains MHY343 and MHY619 express $^{FLAG}\beta$ in a W303 background (Y300 is the parent strain). $^{FLAG}\beta$ contains N-terminal amino acids MDYKDDDDKH from a *FLAG-RNR2* replacement integrated into the genome at the *RNR2* locus under the control of the native *RNR2* promoter. MHY619 was isolated among tetrads that resulted from a genetic crossing between a haploid strain of the *FLAG-RNR2* genotype and a haploid strain of the *crt1::LEU2* genotype. Wild type strain BY4741 and the isogenic *crt1*Δ strain were obtained from Open Biosystems (*35*). Wild type strain PS0799 was obtained from the Sorger laboratory at the Massachusetts Institute of Technology.

Growth and Isolation of $^{FLAG}\beta$ from MHY343. A single colony was used to inoculate a 5 mL YPAD (yeast extract-

peptone-adenine-dextrose) culture, which was grown overnight to saturation at 30 °C. The starter culture was diluted into 10 L of YPAD in a fermentor and grown at 30 °C for 12−18 h with a typical doubling time of 90 min to a final cell density of $1-3 \times 10^7$ cells/mL. Cells were harvested by centrifugation at 7500*g* for 15 min. Typically, 1−2 g of wet cell paste was obtained per liter of cell culture.

All protein purification steps were carried out at 4 °C. The cell pellet (20 g) was resuspended in 160 mL of 50 mM HEPES (pH 7.4), 1 mM EDTA, 100 mM NaCl, and 10% glycerol (buffer A) supplemented with protease and phosphatase inhibitors [25 μg/mL aprotinin, 10 μM (2*S*,3*S*)-3-(*N*-{(*S*)-1-[*N*-(4-guanidinobutyl)carbamoyl]-3-methylbutyl}-carbamoyl)oxirane-2-carboxylic acid (E-64), 0.4 mM 4-(2-aminoethyl)benzenesulfonyl fluoride (AEBSF), 100 μg/mL pepstatin, 100 μg/mL leupeptin, 100 μg/mL chymostatin, 1 mM benzamidine, 30 mM NaF, and 30 mM β-glycerophosphate]. DNase I (2 units/mL of lysate) was added before cell lysis. The cells were lysed by being passed three times through the French press at 14 000 psi. Cell debris was removed by centrifugation at 30000*g* for 30 min. Crude extract was incubated with 1 mL of anti-FLAG agarose for 1 h with gentle agitation. The mixture was transferred to a column which was subsequently washed with buffer A supplemented with a Complete protease inhibitor tablet until the A_{280} was <0.01. $^{FLAG}\beta\beta'$ was eluted from the column with 8 mL of buffer A supplemented with 150 μg/mL 3×-FLAG peptide. Fractions of 500 μL were collected, and the ones containing $^{FLAG}\beta\beta'$, as judged by the visible spectrum characteristic of the diferric-Y• cofactor, were pooled and concentrated with a YM30 Centricon device (Millipore). Excess 3×-FLAG peptide was then removed by either several rounds of dilution and concentration using a Centricon or passage of the isolated $^{FLAG}\beta\beta'$ through a Sephadex G-50 column. The yield of $^{FLAG}\beta\beta'$ ranged from 30 to 75 μg/g of cell paste.

Isolation of $^{FLAG}\beta'$ from MMS-Treated Cells. MHY343 was grown as described above, with the following modifications. When the culture reached a density of 2×10^7 cells/mL, MMS was added to a final concentration of 0.01% (v/v) and the cells were harvested 1.5 h later.

The cell pellet (20 g from a 10 L fermentation) was resuspended in 160 mL of buffer A supplemented with protease and phosphatase inhibitors. $^{FLAG}\beta\beta'$ was isolated as described above except that 1.5 mL of anti-FLAG agarose was used. The column was washed with 600 mL of buffer A followed by elution with 100 μg/mL 3×-FLAG peptide in buffer A. The desired fractions were pooled and concentrated to give 700 μg of $^{FLAG}\beta\beta'$.

Isolation of $^{FLAG}\beta\beta'$ from the MHY619 ($^{FLAG}\beta$-crt1Δ) Strain. MHY619 was grown, and $^{FLAG}\beta\beta'$ (2.7 mg) was isolated from 7.5 g of cell paste (from a 10 L fermentation growth) as described for MHY343. $\beta\beta'$ contained a small amount of DNA contamination (λ_{max} of 276 nm), preventing reliable determination of the protein concentration with the extinction coefficient, and therefore, the protein concentration was determined with a Bradford assay using $^{His}\beta\beta'$ as a standard.

Activity Assay with Purified Subunits. A typical reaction mixture contained, in a final volume of 135 μL, 100 mM HEPES (pH 7.4), 20 mM $MgCl_2$, 6−36 μM α, 0.3 μM $^{FLAG}\beta\beta'$, 3 mM ATP, 1 mM [^{14}C]CDP (specific activity of $1-2 \times 10^3$ cpm/nmol), 100 μM *E. coli* thioredoxin, 1 μM *E. coli* thioredoxin reductase, and 2 mM NADPH (*36*, *37*). Only the data corresponding to $^{FLAG}\beta\beta'$ isolated from the MHY619 strain were assayed with an α concentration greater than 6 μM. The assay mixture was preincubated at 30 °C for 5 min and the reaction initiated by the addition of substrate. Aliquots (30 μL) were removed over the course of 10−20 min and reactions quenched in a boiling water bath. dCDP production was analyzed by the method of Steeper and Stewart (*38*). The specific activity was calculated per milligram of β or $^{FLAG}\beta$.

Preparation of Samples for Whole-Cell EPR Analysis, Quantitative Western Blots, and Specific Activity Measurements. Typically, different strains of *S. cerevisiae* [MHY343, MHY619, BY4741, BY4741-*crt1*Δ, Y300, and PS0799 (Table 1)] were grown in 2 L to mid-log phase ($1-3 \times 10^7$ cells/mL) in YPD (yeast extract-peptone-dextrose) or YPAD at 30 °C. Some of the cells (1.6 L) were collected by centrifugation at 7500*g* for 15 min, washed twice with 1 L of ice-cold phosphate-buffered saline (PBS) and then with 50 mL of ice-cold PBS containing 30% glycerol. The pellets were frozen in liquid nitrogen and stored at −80 °C. As a background control for the EPR experiments, the remaining 0.4 L of the cell culture was treated with 0.15 M hydroxyurea (HU), incubated at 30 °C for an additional 1 h, and then harvested. The pellets were then washed and frozen. For MMS-treated cells, MMS was added to a final concentration of 0.01% (v/v) for the last 1.5 h of cell growth and then harvested as described above.

Whole-Cell EPR. The cell pellet (1.6 g) was resuspended in 1 mL of PBS with 30% glycerol to a final concentration of $1-3 \times 10^{10}$ cells/mL. Part of the suspension (220 μL) was packed directly into calibrated EPR tubes and frozen in liquid nitrogen. A similar workup was carried out on the HU-treated cells (0.4 g). Experiments were performed on three to eight different cultures for each strain and for the corresponding HU-treated cells. EPR spectra were recorded using a Bruker ESP-300 X-band (9.4 GHz) spectrometer equipped with an Oxford liquid helium cryostat to maintain the temperature at 30 K. Typical instrument parameters were as follows: frequency, 9.38 GHz; power, 0.201 and 2.526×10^{-3} mW for the yeast and *E. coli* Y•, respectively. For the $CuSO_4$ standard, the power was 5.029×10^{-2} mW. The standards used for spin quantification were the *E. coli* Y• (1−115 μM) or $CuSO_4$. The R2 concentration was determined using an ϵ_{280} of 131 mM^{-1} cm^{-1}, and Y• content was determined by the drop-line correction method (*39*). The $CuSO_4$ standard was at a concentration of 1.02 mM ($\epsilon_{810} = 11.79$ mM^{-1} cm^{-1}), >99.99% pure, in 2 M $NaClO_4$, 0.01 M HCl, and 20% (v/v) glycerol (*40*).

Cell Counting. Subsequent to the EPR analysis, the samples were thawed and the number of cells was counted using a hemacytometer. For each sample, four to six independent dilutions were made and counted by two different workers, and the average of these numbers, with a standard deviation of 15−20%, was used in data analysis.

EPR Quantification of Y• Content and Removal of the Background EPR Features. Whole-cell EPR spectra of cells with or without HU were normalized to the collection parameters and the number of cells packed into each EPR tube. To obtain a spectrum of Y• only, the spectrum of the HU-treated cells was subtracted from the corresponding EPR

spectrum of untreated cells. The total spin concentration was determined by double integration of the difference spectrum and analyzed relative to the standard curve of $Y^{\bullet}$ of *E. coli* R2 and $CuSO_4$. The in vivo concentration of $Y^{\bullet}$ was determined using the number of cells per milliliter from cell counting and a volume of 70 fL for MHY343, MHY619, Y300, and PS0799 cells and a volume of 42 fL for BY4741 and BY4741-*crt1*Δ cells (*41*, *42*) (see the Supporting Information for the equation used). Cell volumes were measured using a Coulter Counter or by measuring the size of the yeast using electron microscopy images (*41*, *42*). EPR spectra of purified $^{FLAG}\beta\beta'$ samples were recorded at ~10 μM, and the concentration of $Y^{\bullet}$ was determined relative to the standards.

Crude Extract Preparation for Western Blot Analysis and Determination of the Specific Activity of $\beta\beta'$. The remainder of the resuspended cell pellet (780 μL) described in the cell growth section above was used to prepare extracts for quantitative Western blots and specific activity determinations. All steps were carried out at 4 °C. The suspension was diluted to ~8.5 mL with 50 mM Tris-HCl (pH 7.9), 5% glycerol, 10 mM $MgCl_2$, 300 mM $(NH_4)_2SO_4$, 1 mM EDTA, 1 mM DTT, 25 μg/mL aprotinin, 10 μM E-64, 0.4 mM AEBSF, 100 μg/mL pepstatin, 100 μg/mL leupeptin, 100 μg/mL chymostatin, 1 mM benzamidine, 10 mM NaF, 100 mM β-glycerophosphate, and DNase I (5 units/mL lysate) (buffer B). An aliquot (10 μL) of the diluted mixture was removed and the number of cells per milliliter determined using a hemacytometer. The remainder of the sample was then lysed by three to four passes through the French press (14 000 psi). An additional aliquot of cells (10 μL) was removed after lysis to determine the efficiency of cell cracking. Cell debris was removed by centrifugation (30000*g* for 30 min), and the protein concentration was determined by the Bradford assay using BSA as the standard. A portion of this extract (400 μL) was diluted into 2× Laemmli buffer, frozen in liquid nitrogen, and stored at −80 °C until Western blot analyses were performed. The remainder of the extract (~8.1 mL) was used directly for partial purification and specific activity determination as described below.

Western Blotting of Crude Cell Extracts. For Western blot analyses, a purified $^{His}\beta$ standard (1−7 ng) and various crude extracts (0.1−8 μg) were run on a 10% SDS−PAGE Tris-HCl gel (Bio-Rad Criterion Gel). The $^{His}\beta$ standard was mixed with 5 μg of crude cell extract from *E. coli* BL21-(DE3)-Gold cells (0.42 mg/mL) and the concentration of unknowns optimized for each extract so that they fell within the standard curve range. Low protein binding tips (Axygen) and Eppendorf tubes (Axygen) were required to generate reproducible standard curves. Protein was transferred to a PVDF membrane (Immun-Blot PVDF, Bio-Rad) using a tank transfer unit in transfer buffer (25 mM Tris, 192 mM glycine, 15% methanol, and 0.01% SDS at 4 °C) at 200 mA for 60 min. As a control, a second membrane was added to ensure that no overtransfer of β occurred. Furthermore, the gel, subsequent to transfer, was silver-stained to ensure that all β was transferred. Polyclonal Abs to $^{His}\beta$ were isolated as previously described and were used at a 1:10000 dilution, while the secondary Abs were used at a 1:5000 dilution (*30*). Detection of β was carried out as described except that the blots were developed with the DuraWest Chemiluminescent Reagent (Pierce) (*28*). The chemiluminescent signal was detected with a CCD camera (ChemiDoc XRS, Bio-Rad), and the band intensities were quantified using Bio-Rad's Quantity One software. The standard curve was generated from a plot of variable amounts of purified $^{His}\beta$, including the control with no $^{His}\beta$ (background signal). The data were analyzed using a linear fit weighted against the standard deviation of each of the measured band intensities, and the resulting line was used to calculate the unknown concentration of β in each of the cell extracts (Figure 1 of the Supporting Information). For each extract, duplicates of four different concentrations were examined. Cell counting and cell volumes described above were used to calculate the concentration of β (see the Supporting Information for the equation used).

Specific Activity Determination of β *and* $^{FLAG}\beta$ *from Partially Purified Extracts.* The supernatant from the lysed cells described above (~8.1 mL) was used immediately. DNA was removed by the dropwise addition of polyethyleneimine (2% stock solution adjusted to neutral pH) to a final concentration of 0.2%. The precipitate was removed by centrifugation (40000*g* for 20 min), and the supernatant was treated with solid ammonium sulfate to 65% saturation (430 mg/mL). The precipitated proteins were collected by centrifugation (40000*g* for 20 min). The protein pellet was dissolved in a minimal volume of buffer B (~1 mL) and desalted with a Sephadex G-50 column (0.7 cm × 16 cm) equilibrated in 25 mM HEPES (pH 7.2), 25 mM $MgSO_4$, 50 mM $(NH_4)_2SO_4$, and 5% glycerol supplemented with a Complete protease inhibitor tablet. The protein concentration was determined by the Bradford assay using BSA as the standard. The partially purified extract was used immediately in the activity assay without freezing. The entire procedure from the time the cells were cracked until the assay was performed took 3.5−4 h. Freezing and storage at −80 °C were found to decrease the activity of β in extracts. An aliquot of protein was also diluted 2-fold with 2× Laemmli buffer, immediately frozen in liquid nitrogen, and stored at −80 °C for later use in Western Blot analysis following the protocol described above.

The partially purified crude extract assays were identical to the assays described above for purified $^{FLAG}\beta\beta'$ except that they contained 0.25−2 mg/mL (total crude protein) extract, 1 mM [^{14}C]CDP (~5000 cpm/nmol), and 10 mM NaF. All components except the extract were mixed and preincubated at 30 °C for 5 min. The assay was initiated by the addition of extract that was also equilibrated to 30 °C. The specific activity was calculated per milligram of β or $^{FLAG}\beta$ after determining the subunit concentration used in each assay by the Western blot procedure.

RESULTS

Rapid Isolation of $^{FLAG}\beta\beta'$ *from S. cerevisiae*. Our first approach to determining R2's cofactor stoichiometry in vivo was to develop a method for the rapid isolation of R2 without overexpression from a wt strain. Yeast strain MHY343, with a genomically tagged β consisting of an amino-terminal fusion of the FLAG epitope under control of the *RNR2* promoter, was constructed for this purpose. The N-terminus of β was chosen as the site of tag attachment, as the C-terminus is required for R1−R2 interaction (*43*, *44*). Recent studies with several different N-terminally His-tagged β constructs have demonstrated that activity is subtly

Table 2: Summary of the Results Obtained from the $^{FLAG}\beta\beta'$ Isolations

strain	yield of $^{FLAG}\beta\beta'$ (μg/g of cell paste)	specific activity [nmol min^{-1} (mg of β)$^{-1}$]	iron content (no. of irons per $^{FLAG}\beta\beta'$)	Y$^{\bullet}$ content (Y$^{\bullet}$/$^{FLAG}\beta\beta'$)
MHY343	40	2306 ± 481[a]	1.45 ± 0.05	0.45 ± 0.08
MHY343 (MMS-treated)	35	2100[a]	1.6	0.5
MHY619	360	3188, 3379[b]	ND[c]	0.5 ± 0.05

[a] $^{FLAG}\beta\beta'$ activity measured using 0.3 μM $^{FLAG}\beta\beta'$ and 6 μM α. [b] $^{FLAG}\beta\beta'$ activity measured using 0.3 μM $^{FLAG}\beta\beta'$ and either 12 or 36 μM α. [c] Not determined.

Table 3: In Vivo Concentration of Y$^{\bullet}$ and β or $^{FLAG}\beta$ Determined by Whole-Cell EPR and Western Blot Analysis[a]

strain	Y$^{\bullet}$ (μM) (no. of times measured)	β or $^{FLAG}\beta$ (μM) (no. of times measured)	Y$^{\bullet}$/$\beta\beta'$ or Y$^{\bullet}$/$^{FLAG}\beta\beta'$
BY4741 (β)	0.89 ± 0.11 (5)	1.07 ± 0.07 (4)	0.83 ± 0.10
BY4741 and MMS (β)	3.19 ± 0.19 (4)	5.78 ± 1.24 (4)	0.55 ± 0.08
BY4741-*crt1*Δ (β)	14.90 ± 1.34 (8)	30.71 ± 6.08 (4)	0.49 ± 0.05
PS0799 (β)	0.66 ± 0.10 (4)	0.74 ± 0.09 (4)	0.89 ± 0.15
PS0799 + MMS (β)	2.27 ± 0.11 (4)	4.40 ± 0.51 (6)	0.52 ± 0.06
Y300 (β)	0.86 ± 0.03 (4)	0.98 ± 0.04 (4)	0.88 ± 0.03
Y300 + MMS (β)	2.82 ± 0.37 (4)	3.89 ± 0.90 (4)	0.72 ± 0.13
MHY619 ($^{FLAG}\beta$, *crt1*Δ)	6.16 ± 0.62 (6)	10.89 ± 2.05 (4)	0.57 ± 0.09
MHY343 ($^{FLAG}\beta$)	0.40 ± 0.20 (11)	0.31 ± 0.07 (4)	1.30 ± 0.72

[a] All the numbers reported in the table are the average numbers obtained over the number of trials indicated ± the standard deviation of those trials.

dependent on the construct (*15*, *28*, *45*). Thus, MHY343 cells were examined for growth rate and sensitivity to genotoxic stress as a course monitor of tag effects. The cell doubling time was 5−10 min longer than that of the wt strain, and their appearance was similar to that of the wt strain except that they had a slightly greater tendency to clump. MHY343 cells subjected to genotoxic stress induced by 50 mM HU show no obvious growth defect relative to the wt strain on solid YPD medium (data no shown). Finally, $^{FLAG}\beta$ shows the same nucleus to cytoplasm shuttling seen with wt β in response to S-phase or genotoxic stress (M. Huang, unpublished results, and ref *46*). Thus, the presence of the 10-amino acid tag does not grossly affect β function in vivo.

Immunoaffinity chromatography with Abs to the FLAG epitope allowed isolation of $^{FLAG}\beta\beta'$ from MHY343 cells within 3.5−4 h of cell disruption. SDS−PAGE of $^{FLAG}\beta\beta'$ isolated from three independent experiments revealed a >90% purity, as judged by Coomassie staining (data not shown). The $\epsilon_{280-310}$ for apo-$^{His}\beta\beta'$ was used to determine the concentration of $^{FLAG}\beta\beta'$, where $\epsilon_{280-310}$ is an average ϵ (99 800 M^{-1} cm^{-1}) for $^{His}\beta_2$ and β' (*28*). This ϵ is within 2−4% of the theoretical ϵ (95 480 M^{-1} cm^{-1}) and that previously determined by Thelander and co-workers (102 000 M^{-1} cm^{-1}) (*15*). Studies with *E. coli* R2 revealed that the extinction coefficient of its apo and holo forms differ by ∼8% [121 vs 131 mM^{-1} cm^{-1}, respectively (*47*)]. Thus, a reasonable error associated with determination of the concentration of $^{FLAG}\beta\beta'$ using this method is ∼8%. The average specific activity from these isolations was 2.3 ± 0.5 μmol min^{-1} mg^{-1} with average iron and Y$^{\bullet}$ contents of 1.45 ± 0.05 and 0.45 ± 0.08, respectively (Table 2). The measured specific activity was a little lower than expected and is thought to be a result of not saturating $^{FLAG}\beta\beta'$ activity with α. The visible spectrum of $^{FLAG}\beta\beta'$ is indistinguishable from that of $^{His}\beta\beta'$ obtained by reconstitution of the cluster from $^{His}\beta_2$ and β'_2 isolated from *E. coli* (data not shown). The spectrum of the Y$^{\bullet}$ cofactor resembles those previously reported for mouse, *Arabidopsis*, and vaccinia virus R2 (*48*−*50*).

Isolation of $^{FLAG}\beta\beta'$ from MMS-Treated Cells. These results demonstrate that even with the rapid isolation of $^{FLAG}\beta\beta'$, the amounts of Y$^{\bullet}$ are still substoichiometric (Table 2). One rationalization of this observation is that cells have evolved a pathway not only to assemble the diferric-Y$^{\bullet}$ cofactor but also to specifically modulate (reduce and regenerate) the Y$^{\bullet}$ as a mechanism of regulation of RNR activity in vivo. A system may exist in *S. cerevisiae*, similar to that characterized in *E. coli* crude extracts, that can generate met-R2 (R2 with a reduced Y$^{\bullet}$ and the diferric cluster intact) and can regenerate holo-R2 from met-R2 (*19*−*21*, *51*−*53*). Furthermore, the population of cells from which $^{FLAG}\beta\beta'$ was isolated was asynchronous, and consequently, only ∼30% are in the S-phase (*54*). Thus, the $^{FLAG}\beta\beta'$ isolated from this culture may consist of a heterogeneous population of R2s, some which may have 1 Y$^{\bullet}$ per β (present in cells in the S-phase) and others with no radical (present in cells outside of the S-phase). Altering the Y$^{\bullet}$/$^{FLAG}\beta\beta'$ ratio under growth conditions in which RNR activity is elevated would provide support for this model. Thus, MHY343 cells were treated with MMS (0.01%, 1.5 h) to induce a DNA damage response, and the $^{FLAG}\beta\beta'$ protein was isolated. Its purity was similar to that isolated from MHY343 without MMS treatment. $^{FLAG}\beta\beta'$ also contained comparable amounts of Y$^{\bullet}$ and iron and had a specific activity of 2100 nmol min^{-1} (mg of $^{FLAG}\beta$)$^{-1}$ (Table 2). Despite the 4-fold increase in the amounts of β and β' under these growth conditions (Table 3; β' data not shown), the amount of Y$^{\bullet}$/$^{FLAG}\beta'$ is almost identical to that of untreated cells.

Isolation of $^{FLAG}\beta\beta'$ from the MHY619 ($^{FLAG}\beta$, crt1Δ) Strain. An additional way to perturb $\beta\beta'$ levels is the deletion of the transcriptional repressor gene *CRT1* leading to the upregulation of mRNA levels of both β and β' (*31*, *32*). Thus, $^{FLAG}\beta\beta'$ was isolated from MHY619 cells (Table 1). The amount isolated (Tables 2 and 3) was 9-fold higher than the amount routinely isolated from MHY343. $^{FLAG}\beta\beta'$ was again homogeneous as determined by SDS−PAGE and contained 0.5 ± 0.05 Y$^{\bullet}$/$^{FLAG}\beta\beta'$. Interestingly, while both β and β'

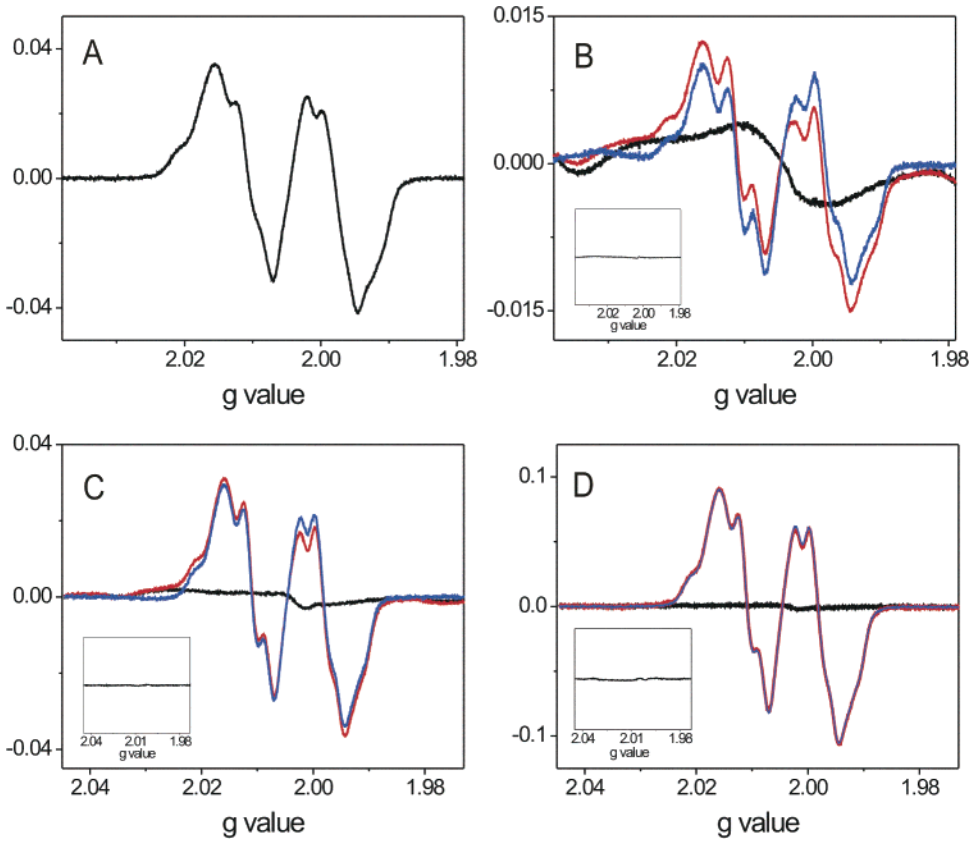

FIGURE 1: EPR spectrum of Y• from purified $^{His}\beta\beta'$ and whole-cell EPR spectra of Y• from BY4741 cells grown in the presence or absence of MMS and BY4741-*crt1*Δ cells. (A) EPR spectrum of Y• from 10 μM $^{His}\beta\beta'$ containing ~0.4 Y•. (B−D) Whole-cell EPR spectra of Y• from (B) BY4741 cells, (C) BY4741 cells treated with 0.01% MMS, and (D) BY4741-*crt1*Δ cells. EPR spectra collected from whole cells are colored red; those for the same cells treated with 150 mM HU for 1 h are colored black, and the results of the subtraction of these two spectra are colored blue. All of the spectra were normalized so that the difference in peak height reflects the differences in spin concentration. The insets show the subtraction of two background spectra from two independent growths of the same strain.

are induced in a *crt1*Δ background, cofactor loading is comparable to that observed in the MHY343 strain.

*Characterization of Y•/ββ′ in Y300, BY4741, and PS0799 Cells Grown in the Presence or Absence of MMS, and of BY4741-crt1*Δ*, and MHY619 Cells by Whole-Cell EPR and Western blotting.* The observed similarities in the Y•/$^{FLAG}\beta\beta'$ ratio under three sets of growth conditions caused us to be concerned about the effects of the FLAG tag on diferric-Y• cofactor assembly in vivo. The aspartates and histidines in the tag could potentially bind iron and interfere with iron binding or delivery of the reducing equivalent to $\beta\beta'$ (*55*). Thus, we have sought an alternative way to measure the Y• levels in vivo. Previous studies by Harder and Follmann in budding yeast suggested whole-cell EPR might be successful (*56*). The Y•/$\beta\beta'$ ratios could then be determined without any perturbation induced by epitope tagging, if the levels of $\beta\beta'$ in crude cell extracts could be quantified using Abs to β. The key to the successful outcome of this approach was determination of the error associated with the measurements and the number of times the experiment was performed.

Whole-cell EPR measurements were taken of Y300, PS0799, and BY4741 strains grown in the presence or absence of MMS as well as in the MHY619 and BY4741-*crt1*Δ strains of *S. cerevisiae* (Table 1). In the MMS-treated and *crt1* strains, the levels of β are elevated up to 30-fold (Table 3). A spectrum of the Y• in reconstituted $^{His}\beta\beta'$ is shown in Figure 1A and serves as a reference point for the whole-cell experiments. Typical spectra of the Y• in whole cells of BY4741, BY4741 grown in the presence of MMS, and BY4741-*crt1*Δ are shown in panels B−D of Figure 1 (red), respectively. Analysis of the low-field region of each whole-cell spectrum reveals broad features not associated with Y• (compare panel A with panels B−D). The endogenous paramagnetic species in the whole cells, even after extensive washing of the cells prior to analysis, potentially complicates quantification of the amount of Y•. A comparison of spectra in panel B or C with that in panel D reveals that when β is elevated 30-fold relative to the isogenic wt strain, the Y• is the predominant feature. To obtain the spectrum of the background paramagnetic species, a portion of each culture was treated with 150 mM HU for 1 h at 30 °C (black, Figure 1B−D). Time course experiments revealed that these conditions are sufficient to reduce the Y•, leaving behind the feature(s) that must be subtracted from the spectrum acquired from untreated cells, to quantify the Y•. The spectra acquired from cells before and after HU treatment were normalized for differences in the collection parameters and the number of cells and the two spectra subtracted. The subtracted spectrum is colored blue in each panel (Figure 1B−D) and looks very similar to the spectrum of Y• of homogeneous $^{His}\beta\beta'$ (Figure 1A). The concentration of Y• was determined by double integration of the subtracted spectrum from a comparison to a standard curve generated using Y• of *E. coli* R2 and a $CuSO_4$ standard. The quantification of Y• was repeated 4−11 times for each strain and condition examined (see Table 3). In addition, to ensure

that the paramagnetic contaminant could be reproduced with each growth, the background spectra generated in different experiments using the same strain were subtracted. The results of typical subtractions are shown in the insets (black) within each panel (Figure 1B−D). While it is apparent from the comparison of the background features that different strains have different background contributions to the overall signal, the flat line in the inset reveals that the background species are produced at the same level when two experiments with the same strain are compared. With the exception of the MHY343 strain, the error associated with measuring the concentration of Y• ranges from 10 to 15% (Table 3).

Cell counting is another key component in the calculation of the Y• concentration in vivo and also has an error associated with it that must be assessed. Typically two different workers counted cells from eight different samples, and the results were averaged. This analysis gives rise to an error of ±20%. Calculation of the concentration of Y• in each strain assumed a volume of 70 fL for Y300, MHY619, and PS0799 cells and a volume of 42 fL for BY4741 cells (*41*). BY4741, Y300, and PS0799 cells have 0.66−0.89 μM Y•, while the strains with *CRT1* deleted have a Y• concentration in the range of 6−15 μM Y• (Table 3). The Y• concentration (micromolar) reported in Table 3 is an average of the number of trials indicated ± the standard deviation from those trials to reflect the reproducibility in obtaining the Y• concentration for each strain. A representative data set for the wt strains is presented in Table 1 of the Supporting Information to show the variability observed in the Y• concentrations.

Whole-Cell EPR with MHY343. Whole-cell EPR experiments were also carried out with the MHY343 strain (Figure 2 of the Supporting Information). In this strain, the background level of the paramagnetic species is substantially higher than that observed in Figure 1B−D. In addition, we were unsuccessful at obtaining reproducible backgrounds between separate growths (see the inset of Figure 2 of the Supporting Information). Determination of the in vivo concentration of Y• in this strain was therefore much more problematic. We tried to reduce the background level of the paramagnetic contaminant(s) by subjecting the cells to additional washes with ice-cold PBS buffer and sonication. We also measured the Y• content of this strain in eight independent experiments (representative data summarized in Table 3). The level of Y• is 0.4 ± 0.2 μM, precluding meaningful analysis of the Y•/$\beta\beta'$ ratio with this strain. Thus, the background levels of the additional paramagnetic species make quantitative analysis impossible even though the Y• is detectable at low levels of β (<0.4 μM).

Western Analysis of Crude Extracts and Determination of Y•/$\beta\beta'$ Ratios. Western blotting potentially allows for determination of the amount of β in crude cell extracts. This number is essential for determination of the Y•/$\beta\beta'$ ratio. This method, in our hands, is associated with significant error; however, the reproducibility in the final measured β concentration was high (see Table 1 of the Supporting Information). The problems encountered and the solutions are thus described in some detail. First, the analysis is dependent on a standard curve for which we used $^{His}\beta$. As noted earlier, this protein is not very stable, and thus, it was critical to use freshly isolated $^{His}\beta$ whose concentration was redetermined before each experiment (*15*, *28*, *45*). The standard curve contained 1−7 ng of $^{His}\beta$ supplemented with 5 μg of *E. coli* BL21(DE3)-Gold crude extract. The addition of this extract facilitated transfer of $^{His}\beta$ to the PVDF membrane in a fashion similar to that of the crude cell extract samples of interest. Since β is essential, a yeast extract lacking β could not be used. Second, experimental conditions were optimized to ensure that all the β from the crude cell extracts and the standards were completely transferred from the gel to the PVDF membrane and that it was not overtransferred through the membrane. In the former case, silver staining of the SDS gel was unable to detect residual β, while in the latter case, multiple membranes were used and no overtransfer was observed. A concentration of 0.01% SDS, as well as exact blotting conditions, was key to the success of quantitative transfer to the PVDF membrane. The amount of crude cell extract analyzed for each strain was chosen to ensure that the amount of β always fell within the 1−7 ng range of the standard curve. Thus, differing amounts of crude cell extract were loaded on the basis of the yeast strain and the growth conditions that were used. When the amounts of β in the crude cell extracts were <0.1 μg, smearing of β became a problem, and thus, these conditions were avoided. The standard and unknown samples were always made in the same buffer to ensure uniform salt conditions, which can also affect protein transfer. Finally, each strain was grown three to eight times, and four different concentrations of crude extract were analyzed with duplicates for each growth. The results of a typical Western blot analysis for BY4741, BY4741 with 0.01% MMS, and BY4741-*crt1*Δ are shown in Figure 2A. In the generation of the standard curve, each concentration of β had its own error and this error as well as a background point was used in generating the final linear fit (Figure 1 of the Supporting Information). The error associated with these determinations using the duplicates of four different concentrations ranged from 3 to 23% (Table 3). The final β concentration (micromolar) reported in Table 3 is the average of the number of trials indicated ± the standard deviation of the various trials. A representative data set for the wt strains is presented in Table 1 of the Supporting Information to show the variability observed in the β concentrations.

Knowing the amount of Y• from the whole-cell EPR experiments and the amount of β from Western blotting, we determined the Y•/$\beta\beta'$ ratio and the error associated with this calculation. Propagation of the error associated with the EPR, Western blot analysis, and cell counting gave Y•/$\beta\beta'$ ratios with an error of 30%. However, since each strain was examined at least four times, the final Y•/$\beta\beta'$ ratio presented in Table 3 is an average of those trials ± the standard deviation to emphasize the reproducibility in obtaining these final numbers. The Y•/$\beta\beta'$ ratio for the wt strains is 0.83−0.88, while the ratio is reduced to 0.49−0.72 in MMS-treated or *crt1*Δ strains. The ratio of approximately 0.5 for both *crt1*Δ strains (MYH619 and BY4741-*crt1*Δ) suggests that the FLAG epitope may not be responsible for the incomplete cofactor loading measured with the isolated $^{FLAG}\beta\beta'$ protein (Table 2). A larger standard deviation is associated with studies on the MHY343 strain (55%), as discussed above. In this case, due to high background levels of paramagnetic species in whole-cell EPR experiments, we are unable to distinguish 0.5 from 1.0 Y•.

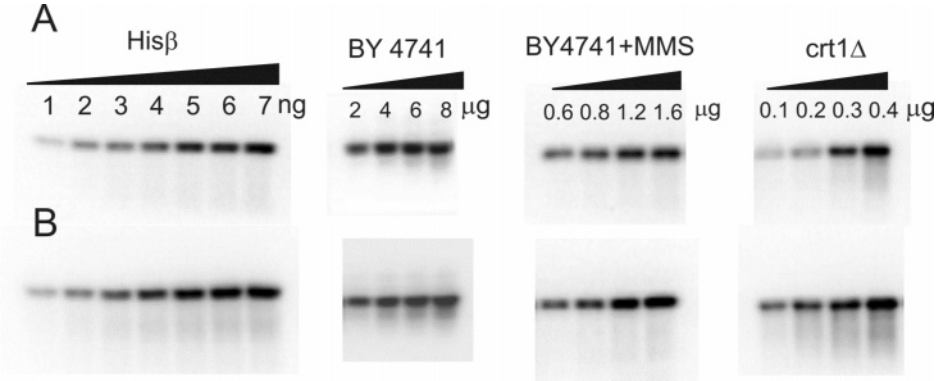

FIGURE 2: Quantitative Western blotting to determine the concentration of β in BY4741, BY4741 with 0.01% MMS, and BY4741-*crt1*Δ. (A) Western blots of the crude extracts. (B) Western blots of the partially purified crude extracts. A representative standard curve [1−7 ng with 5 μg of *E. coli* BL21(DE3)-Gold crude extract] generated with freshly purified $^{His}\beta$ is also shown. The total amount of crude extract (micrograms) used for each unknown is indicated above the lane.

Correlation of Y• Content with $\beta\beta'$ Specific Activity. The error associated with determining the Y•/$\beta\beta'$ ratio caused us to seek an independent measurement of this ratio. Previous studies with *E. coli* R2 have demonstrated that its specific activity is proportional to the Y• content when R2 is saturated with R1. Thus, we sought to determine if the same relationship exists between the activity of the *S. cerevisiae* RNR and the Y• content of $\beta\beta'$; if so, this relationship would establish an independent determination of the Y•/$\beta\beta'$ ratio. Using data acquired from numerous reconstitutions of $^{His}\beta\beta'$ in our laboratory as well as data acquired from the isolation of the $^{FLAG}\beta\beta'$ proteins reported herein (Table 2), we see a direct correlation between the amount of Y• and the specific activity of $^{His}\beta\beta'$ and $^{FLAG}\beta\beta'$ within the range of 0.1−0.5 Y• [Figure 3 (●, ▲, ▼, and □)]. The $^{FLAG}\beta\beta'$ isolated from yeast crude extracts has activity comparable to that of our in vitro reconstituted $^{His}\beta\beta'$ when corrected for the amount of Y•. This correlation suggests that if we could determine the activity of $\beta\beta'$ without the tag in crude cell extracts it would be an indicator of Y• loading.

In our initial characterization of $^{His}\beta\beta'$ reconstituted from apo-$^{His}\beta_2$, β'_2, Fe^{2+}, O_2, and reductant, we reported that $^{His}\beta\beta'$ contained 0.6−0.8 Y• and had a specific activity of 0.8−1.3 μmol min^{-1} mg^{-1} (*28*). Those results differ substantially from the experiments reported here and in our subsequent studies with $^{His}\beta\beta'$. The Y• quantification in the initial study was carried out with a 140 GHz spectrometer, while the values reported here were acquired at 9 GHz. We believe our earlier reported quantification of Y• was in error; however, the experimental basis for this error is still unclear as both methods utilized the Y• of *E. coli* R2 to generate the standard. To ensure the spin quantification at 9 GHz is accurate in these studies, a second spin standard, Cu^{2+}, has been used. The radical contents of the heterodimer predicted using these two different standards agree within a few percent.

Determination of β and $^{FLAG}\beta$ Specific Activity with CDP Reduction Assays Using Partially Purified Yeast Extracts. As revealed in Figure 3, determination of the specific activities of purified β and $^{FLAG}\beta$ appears to provide an independent measure of the Y•/$\beta\beta'$ and Y•/$^{FLAG}\beta\beta'$ ratios. Thus, if $\beta\beta'$ activity in crude cell extracts can be measured, then its specific activity would be an indicator of the Y• concentration. Previous studies by Harder and Follmann with crude extracts of baker's yeast and our own studies with *S. cerevisiae* have demonstrated that the measurement of RNR activity in crude extracts is challenging (*56*). The difficulty was initially thought to be associated with metabolism of substrates and allosteric effectors. However, we now believe that the difficulty is in part related to our lack of understanding of how protein concentration and the presence of nucleotides influence the oligomeric state of α and the interaction between α_n and $\beta\beta'$. To break the cell walls of yeast efficiently, ~8 mL of buffer is required per gram of cells leaving both α_n and $\beta\beta'$ at low levels in the crude extracts (~0.005 μM). The K_D for the interaction between α_n and $\beta\beta'$ in *S. cerevisiae* has yet to be precisely determined; however, in *E. coli* and mouse, the K_D for the interaction between α_2 and β_2 is in the range of 0.2 μM (without nucleotides) (*15*). Thus, the crude extracts were partially

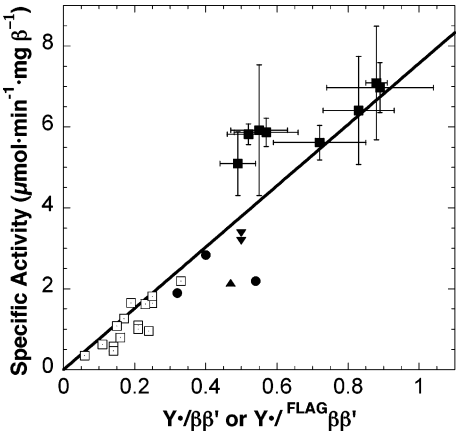

FIGURE 3: Correlation of the Y•/$\beta\beta'$ ratio and the specific activity of β using β, $^{FLAG}\beta$, or $^{His}\beta$. Results from several in vitro reconstitutions of $^{His}\beta\beta'$ (□) are plotted along with $^{FLAG}\beta\beta'$ isolated from the MHY343 strain (●), the MHY619 strain (▼), and the MHY343 strain with 0.01% MMS (▲). The results from the activity assays using the partially purified extracts are also plotted with the standard deviations shown for the assay and for the quantification of Y• by whole-cell EPR spectroscopy (■). The points without error bars were all performed with purified proteins in vitro prior to the correlation analysis. The error in determining the Y• concentration is small since the activity assays and EPR data were collected on purified proteins. Furthermore, the error in measuring the specific activities is also small. However, the specific activities reported should be ~15% greater since all of the experiments, except those corresponding to $^{FLAG}\beta\beta'$ isolated from MHY619, were performed using 6 μM α and 0.3 μM $^{His}\beta\beta'$ or $^{FLAG}\beta\beta'$. We have subsequently shown that β is not saturated under these conditions. An increase of 15% in activity would move most of the in vitro points closer to the line.

Table 4: Specific Activities of Partially Purified Yeast Extracts[a]

strain	specific activity per milligram of total protein in crude extract (nmol min^{-1} mg^{-1})	specific activity per milligram of β or $^{FLAG}\beta$ (nmol min^{-1} mg^{-1})
BY4741 (β)	5.6 ± 1.2	6409 ± 1338
BY4741 and MMS (β)	23.6 ± 0.3	5921 ± 1616
BY4741-*crt1*Δ (β)	118.0 ± 1.6	5095 ± 788
PS0799 (β)	7.7 ± 0.1	6971 ± 618
PS0799 and MMS (β)	33.6 ± 0.6	5821 ± 257
Y300 (β)	7.2 ± 0.1	7090 ± 1406
Y300 and MMS (β)	29.8 ± 0.6	5615 ± 429
MHY619 ($^{FLAG}\beta$, *crt1*Δ)	36.0 ± 0.1	5867 ± 351
MHY343 ($^{FLAG}\beta$)	4.3 ± 0.1	10542 ± 2567

[a] All the data reported in Table 4 are the average numbers obtained over at least four trials ± the standard deviation of those trials.

purified for the RNR activity measurements to concentrate the RNR subunits and to avoid nucleotide metabolism.

The CDP reduction activities of partially purified extracts from BY4741, Y300, and PS0799 cells grown in the presence or absence of MMS, and of MHY343, and MHY619 cells were determined for $\beta\beta'$ and $^{FLAG}\beta\beta'$ by titration with α_n until a maximal activity was obtained. The amount of protein was determined by either the Bradford assay using BSA as a standard or quantitative Western blotting using Abs to the $^{His}\beta$ protein (Figure 2B). The results have allowed calculation of specific activities either per milligram of total protein in crude extract or per milligram of β (or $^{FLAG}\beta$) as shown in Table 4. When the specific activities per milligram of total protein were compared, the MHY619 strain has 5-fold more activity than its parental wt strain (Y300) and 8-fold more activity than the MHY343 strain, while the BY4741-*crt1*Δ strain has 21-fold more activity than its parental wt strain (BY4741). The lower specific activities of the MHY343 and MHY619 strains compared to the BY4741 and BY4741-*crt1*Δ strains suggest that although the FLAG tag does not affect the function of β in vivo, it appears to affect the expression of β.

As mentioned above, the specific activity per milligram of β or $^{FLAG}\beta$ was determined using quantitative Western blotting. Errors of 20−30% between individual Western blots of the same extract were typically observed; however, the standard deviation of the final β concentration measured after at least four trials was analogous to what is reported in Table 3 (see the Supporting Information). The results reveal that the specific activity of β is approximately 6800 nmol min^{-1} mg^{-1} for all the wt strains (BY4741, Y300, and PS0799) examined. The specific activities for these strains can now be added to the data in Figure 3 and for the first time provide insight into the specific activity of β with "high" radical loading (>0.5 Y$^{\bullet}$). Extrapolation of the data gives a specific activity for β with ∼1 Y$^{\bullet}$ of 7500 nmol min^{-1} (mg of β)$^{-1}$, a value substantially higher than any activities previously reported for eukaryotic RNRs [250−2500 nmol min^{-1} (mg of β)$^{-1}$] and strikingly similar to the activity of *E. coli* R2 (*15*, *57*, *58*). This independent method thus supports the conclusion that $\beta\beta'$ can be completely loaded with cofactor in vivo in the wt strains.

Does α_n or $\beta\beta'$ Limit RNR Activity? On the basis of mRNA levels, previous studies have suggested that α, and not $\beta\beta'$, limits RNR activity in vivo (*22*, *59*). Thus, to understand why the levels of active $\beta\beta'$ have been elevated when wt cells are subjected to MMS treatment, the levels of α, α′, β, and β' were measured by Western blot analysis using the appropriate Abs under one set of conditions: BY4741 cells grown in the presence or absence of MMS (Table 5). In the absence of MMS, the concentration of α was 0.7 μM while no α′ was detected, and the levels of both β and β' were approximately 0.8 μM. Therefore, under normal growth conditions, α and $\beta\beta'$ are present in equimolar amounts in a population of asynchronously grown cells. However, in MMS-treated cells, there was a 3-fold increase in the amount of $\beta\beta'$ relative to α: the level of α rose to 1.0 μM and the levels of β and β' each rose to approximately 3.0 μM. Interestingly, α′ levels rose to 0.4 μM; however, the contribution of α′ to RNR activity under these conditions remains unknown (*23*). Given that the specific activity of β is approximately 10 times greater than that of α (see the Discussion) and that α and $\beta\beta'$ are present in equimolar amounts in untreated cells, it is surprising that the $\beta\beta'$ levels are elevated to twice that of the α plus α′ levels in cells treated with MMS.

Table 5: RNR Subunit Concentrations and Specific Activity of Crude Extracts from BY4741 Cells Grown in the Presence or Absence of MMS

strain	Western analysis[a] [β] (μM)	[β'] (μM)	[α] (μM)	[α′] (μM)
BY4741	0.82	0.50	0.70	<0.0
BY4741 and MMS	3.02	3.19	1.01	0.43

strain	specific activity [nmol min^{-1} (mg of total protein in extract)$^{-1}$][b] crude extract	crude extract and 6 μM α	crude extract and 3 μM $^{His}\beta\beta'$[c]
BY4741	0.07	3.7	0.25
BY4741 and MMS	0.44	8.5	0.59

[a] Western analysis performed using blotting conditions described previously (*14*). [b] Activity assays performed using 2−5 mg/mL crude extract and using 30 mM DTT as the reductant. Note these assays differ from those described in Materials and Methods (Table 4). [c] $^{His}\beta\beta'$ reconstituted by in vitro methods which has ∼0.2 Y$^{\bullet}$/$^{His}\beta\beta'$.

The crude extracts of the two strains (BY4741 grown in the presence or absence of MMS) were also assayed for dCDP production as an independent check of which subunit limits RNR activity. The results of assaying each subunit in the absence and presence of either 6 μM α or 3 μM $^{His}\beta\beta'$ are also shown in Table 5. Addition of excess $\beta\beta'$ to the crude extracts of each strain has little effect on the activity. The specific activity of BY4741 increases 3.2-fold from 0.07 to 0.25, while the activity of BY4741 with MMS increases 1.3-fold from 0.44 to 0.59. However, the addition of α to crude extracts results in a dramatic increase in activity, more than 50-fold for BY4741 and almost 20-fold in the presence of MMS, consistent with α activity being limiting. Thus, the elevated levels of $\beta\beta'$ in response to DNA-damaging agents are intriguing, as sufficient $\beta\beta'$ is already present in the BY4741 strain to saturate α activity if all the proteins form an active RNR complex.

DISCUSSION

Deoxynucleotide pools are required during the S-phase of the cell cycle when DNA is replicated, and subsequent to cells sensing DNA damage when DNA must be repaired.

Failure to control the relative ratios and the amounts of dNTPs can lead to mutations and, in humans, a predisposition to diseases, including cancers (*60*, *61*). RNRs are a major site of regulation for the control of these pools (*2*, *62*). The common features of RNR regulation are the allosteric effectors that control, in part, the activity and substrate specificity and transcription factors that control the mRNA levels of the subunits as a function of the cell cycle (*24*, *63*−*66*). In eukaryotic systems, a third common regulatory mechanism involves sequestration of the subunits in different compartments within the cell (*46*, *67*, *68*). In many other organisms, specific regulatory mechanisms have also been described. These include the control of RNR activity via modulation of subunit degradation, modulation of the RNR quaternary structure, regulation of R1 activity by interaction with a small protein whose presence is modulated as a function of cell cycle, and control of specific subunit mRNA stability (*6*, *69*−*71*). Integration, spatially and temporally, of these primary control mechanisms of RNR is, in general, not understood in any organism.

S. cerevisiae has served as a model for understanding the control of RNR activity in eukaryotic organisms (*24*, *60*). This organism possesses no deoxynucleoside kinase activities, and thus, dNTP synthesis is entirely dependent on RNR (*72*). In *S. cerevisiae*, the levels of the subunits are controlled transcriptionally and the level of mRNA of the α subunit is increased during the S-phase of the cell cycle during normal growth, while the levels of mRNA for the β and β' subunits remain largely unchanged (*22*, *25*, *27*, *31*). We have recently shown that the mRNA levels are correlated with the protein levels (D. L. Perlstein, M. Huang, and J. Stubbe, unpublished results). Thus, the current model is that in *S. cerevisiae* the rate-limiting step in dNTP production is RNR and that its activity is largely modulated by the concentration of the α subunit (*22*, *59*). This interpretation assumes that $\beta\beta'$ is in excess and is fully loaded with the essential diferric-Y$^\bullet$ cofactor. However, if $\beta\beta'$ is not loaded with cofactor, it could limit nucleotide reduction by modulating the amount of "active" $\beta\beta'$ as a function of cell cycle. In this model, the Y$^\bullet$ concentration, and not the amount of protein, is regulated (*15*, *51*, *73*).

Regulation of RNRs at the level of their quaternary structure is also essential to unravel. RNR activity depends upon a number of complex equilibria that are not understood either in vitro or in vivo. The α subunit can be oligomeric, and the oligomeric state is dependent on dNTP (ATP) binding (*74*). Furthermore, the quaternary structure(s) of active $\alpha_n(\beta\beta')_n$ has (have) not been identified, and the equilibria between subunits are also governed by dNTPs and ATP in a way that is not completely understood. The issue of cofactor loading as a regulatory mechanism of RNR activity in vivo has been resolved by our studies presented in this paper. Our results have also raised new questions about the issue of the enzyme's quaternary structure and its relationship to activity in vivo.

Regulation of Levels of the Diferric-Y$^\bullet$ Cofactor Is Not Involved in Regulation of RNR Activity. The activity of *E. coli* RNR in vitro has been previously shown to correlate with the amount of Y$^\bullet$/R2 (*18*). In this study, we have shown that in *S. cerevisiae* the Y$^\bullet$/$\beta\beta'$ ratio determines the RNR activity in vivo (Figure 3). Previous studies in *E. coli* have suggested that there are protein factors required for initial assembly of the cofactor, as well as maintenance of the cofactor during different stages of cell growth (*51*). In *E. coli*, if the Y$^\bullet$ of R2 is reduced, RNR is inactive. However, the Y$^\bullet$ can be regenerated by reduction of the diferric cluster to a diferrous cluster, followed by reaction with oxygen and a reducing equivalent (*51*). Assembly and disassembly of the diferric-Y$^\bullet$ cofactor in *S. cerevisiae* could potentially provide an additional layer of regulation of RNR activity.

These studies provide the first measurement of the Y$^\bullet$/$\beta\beta'$ ratio and the activity of a fully loaded $\beta\beta'$ subunit from asynchronously growing cells. In the three wt strains that were examined (Tables 3 and 4), the ratio is 0.83−0.88 as measured by two independent methods and the specific activity of a fully loaded $\beta\beta'$ is extrapolated to be ∼7500 nmol min^{-1} mg^{-1}. Thus, changes in the Y$^\bullet$ concentration in the three wt strains are not a modulator of RNR activity, and the amount of $\beta\beta'$ is an indicator of the amount of active $\beta\beta'$.

The Y$^\bullet$/$\beta\beta'$ ratio has also been examined under two additional sets of conditions, both of which result in elevated concentrations of $\beta\beta'$. When the wt strains are treated with the DNA methylating agent MMS, the $\beta\beta'$ levels increase 4−6-fold (Table 3), but the Y$^\bullet$/$\beta\beta'$ ratio decreases to 0.5 relative to that of the untreated wt strain. Thus, there is a 200% increase in the level of active $\beta\beta'$ with 50% of $\beta\beta'$ remaining in the apo form. If α is rate-limiting for deoxynucleotide reduction during this environmental insult, then its levels might be expected to increase under these growth conditions. However, the data in Table 5 indicate that the levels of α increase only slightly from 0.7 to 1.0 μM in the presence of MMS, while α′ levels increase from 0 to 0.4 μM. These data suggest that α remains rate-limiting for deoxynucleotide reduction under DNA-damaging conditions. However, the role of α′ in RNR activity is at present unclear. Domkin et al. have shown in vitro that the activity of α′ is less than 1% of that of α, yet when α′ forms a heterooligomer with α ($\alpha_n\alpha'_n$), the activity of α′ is now 5% of that of α (*23*). Further investigation of the role of α′ and its relationship with active $\beta\beta'$ is ongoing.

With the *crt1* strains, the $\beta\beta'$ levels are elevated 10−30-fold while the Y$^\bullet$/$\beta\beta'$ ratio is again reduced to 0.5−0.6. The levels of $\beta\beta'$ have been artificially elevated due to the deletion of the transcriptional repressor; however, the cellular machinery required to assemble the diferric-Y$^\bullet$ cluster can still assemble up to 15 times the amount of cofactor found in the wt strains. Thus, these extracts are being examined as a starting point for identifying factors involved in diferric-Y$^\bullet$ assembly. Recent microarray analysis of the *crt1*Δ strain showed elevated transcript levels of many genes; however, none of the corresponding proteins were readily identifiable with biosynthetic machinery that might be involved in active cofactor assembly (*32*).

Specific Activity Measurements Suggest that RNR Need Not Be Rate-Limiting in dNTP Formation. Assaying crude cell extracts and purified subunits for RNR activity is associated with many difficulties in all organisms (*62*). In *S. cerevisiae*, for example, activity measured in crude extracts is modulated by the ratio of buffer used per gram of cells required for efficient cell disruption. This ratio can lead to a 5−10-fold dilution of the subunits, potentially resulting in alterations in the oligomeric state of α and the α_n−$\beta\beta'$ interaction. Thus, the activity of α in crude cell extracts is

typically measured in the presence of excess $\beta\beta'$, and the activity of $\beta\beta'$ is measured in the presence of excess α_n. Using this methodology, we have extrapolated from the data presented in Figure 3 that the specific activity of $\beta\beta'$ is ~7500 nmol min^{-1} mg^{-1} for 1 Y$^{\bullet}$/$\beta\beta'$. While similar measurements have not been made for α in vivo, specific activities of α in vitro have been measured to be 350 nmol min^{-1} mg^{-1} in the presence of excess $\beta\beta'$ containing 0.4 Y$^{\bullet}$ (data not shown). The specific activity of α complexed with fully loaded $\beta\beta'$ can then be extrapolated to ~800 nmol min^{-1} mg^{-1}. Recall that α and β have different molecular masses (90 and 43 kDa, respectively), but even if these differences are taken into account, α and β do not have the same turnover number. This observation suggests that these subunit titrations result in different quaternary states of RNRs. The discrepancy in specific activities for α and β has been reported in every class I RNR system examined in detail to date (*57*, *58*, *75*).

In addition to the quaternary structure problem, several other problems are associated with activity measurements. In all eukaryotic systems that were examined, with the exception of our studies, DTT is used as the reductant to allow RNR to catalyze multiple turnovers, rather than the endogenous reductant, thioredoxin and thioredoxin reductase (*76*). In our hands when α is assayed with excess $\beta\beta'$, the activity is reduced several-fold with DTT in place of the protein reducing system (data not shown). When $\beta\beta'$ is assayed with excess α, however, the choice of reductant has little effect. These results suggest that the excess $\beta\beta'$ is interfering with re-reduction of the active site disulfides in a fashion that is not understood. An additional problem is associated with the cofactor loading of R2 and the stability of the loaded cofactor. A number of investigators have reported that the diferric-Y$^{\bullet}$ radical in eukaryotic systems is unstable, and in fact, many investigators include ferric iron and DTT in their assay mixtures (*15*, *77*). Since RNR activity is proportional to the level of Y$^{\bullet}$ (Figure 3), the time elapsed prior to the assay could alter dramatically the RNR turnover number measured due to loss of Y$^{\bullet}$. These problems suggest possible explanations for why the specific activity of α is not equal to the specific activity of $\beta\beta'$ and the large discrepancy in activities between labs. These problems must also be considered when trying to calculate amounts of dNTPs that can be generated by active RNRs.

As noted above, the specific activity of $\beta\beta'$ is ~7500 nmol min^{-1} mg^{-1} and of α_n is ~800 nmol min^{-1} mg^{-1} when $\beta\beta'$ contains ~1 Y$^{\bullet}$. These numbers, the amount of each protein, and the size of the cell under different growth conditions allowed us to calculate the maximum amount of dNTPs that can be generated per cell and how this number relates to the requirements for DNA replication. To replicate the *S. cerevisiae* haploid genome, 2.4×10^7 dNTPs are required and the doubling time is ~90 min. From our data, and the range of specific activities for α_n and $\beta\beta'$, the number of dNTPs produced can be calculated to vary between 3.6×10^8 and 1.1×10^9, a 10−100-fold excess over the requirements for genome replication. Recent dNTP pool measurements by Merrill and co-workers indicate that in asynchronous wt *S. cerevisiae* cells (W303) there are 1.8×10^6 dNTPs, only 10% of the pool size minimally required to replicate the whole genome (*76*). Thus, the low levels of dNTPs measured by Koc et al. suggest that RNR activity is greatly reduced in vivo. At present, there are three mechanisms proposed to regulate RNR activity. One involves the small protein Sml1 that binds to α and causes inhibition by a poorly understood mechanism (*74*, *78*, *79*). The second is feedback inhibition by dATP. Chabes et al. have recently shown that *S. cerevisiae* RNR is 10 times less sensitive to dATP inhibition than the mouse or calf thymus RNRs, requiring 50 μM dATP (with 5 mM ATP present) to observe inhibition in vitro (*23*, *60*). In our crude cell assays described above, the dNTPs have been removed by the ammonium sulfate fractionation and the Sml1 levels are very low due to its low concentrations inside the cell and relatively high K_D with α (~0.4 M) (*74*). The third mechanism is sequestration of α_n and $\beta\beta'$ in different subcellular compartments, thereby decreasing the rate of formation of the active RNR complex [$\alpha_n(\beta\beta')_n$] (*46*). Whether these three modes of inhibition of RNR activity are sufficient to account for the observed relative to the calculated dNTP pool size is not known.

The calculations we have carried out can be extended to our recent studies with an *rnr4*Δ strain in the BY4741 background in which the specific activity of β was found to be 10 nmol min^{-1} mg^{-1}, and the cells were able to still double with a half-life of 180 min (*14*). Under these growth conditions, the amount of β has been elevated 14-fold. A similar calculation of the number of dNTPs produced gives 5.1×10^7, just about enough to replicate the genome.

Whole-cell EPR studies and activity measurements of crude cell extracts provide the first measurement of Y$^{\bullet}$ levels for R2 in vivo. They suggest that in asynchronously growing cells, RNR activity is not modulated at the level of active cofactor formation. Activity measurements and the amounts of α and $\beta\beta'$ in vivo suggest that the subunits are at concentrations much greater than those required for genome replication and that their activities must be greatly modulated to become rate-limiting for DNA replication.

SUPPORTING INFORMATION AVAILABLE

Equations used in the determination of the Y$^{\bullet}$ and β concentrations, a table of representative data obtained in calculating the reported Y$^{\bullet}$ and β concentrations, the standard curve generated for a typical Western blot using known concentrations of $^{His}\beta$ (Figure 1), EPR spectra and Western blots for the MHY343 strain (Figure 2), and EPR spectra and Western blots for all the other strains not shown in the paper (Figure 3). This material is available free of charge via the Internet at http://pubs.acs.org.

REFERENCES

1. Stubbe, J., Ge, J., and Yee, C. S. (2001) The evolution of ribonucleotide reduction revisited, *Trends Biochem. Sci. 26*, 93−99.
2. Jordan, A., and Reichard, P. (1998) Ribonucleotide reductases, *Annu. Rev. Biochem. 67*, 71−98.
3. Kolberg, M., Strand, K. R., Graff, P., and Andersson, K. K. (2004) Structure, function, and mechanism of ribonucleotide reductases, *Biochim. Biophys. Acta 1699*, 1−34.
4. Thelander, L. (1974) Reaction mechanism of ribonucleoside diphosphate reductase from *Escherichia coli*: Oxidation-reduction active disulfides in B1 subunit, *J. Biol. Chem. 249*, 4858−4862.
5. Cooperman, B. S., and Kashlan, O. B. (2003) A comprehensive model for the allosteric regulation of class Ia ribonucleotide reductases, *Adv. Enzyme Regul. 43*, 167−182.

6. Kashlan, O. B., Scott, C. P., Lear, J. D., and Cooperman, B. S. (2002) A comprehensive model for the allosteric regulation of mammalian ribonucleotide reductase. Functional consequences of ATP- and dATP-induced oligomerization of the large subunit, *Biochemistry 41*, 462−474.
7. Scott, C. P., Kashlan, O. B., Lear, J. D., and Cooperman, B. S. (2001) A quantitative model for allosteric control of purine reduction by murine ribonucleotide reductase, *Biochemistry 40*, 1651−1661.
8. Sjöberg, B. M., Reichard, P., Gräslund, A., and Ehrenberg, A. (1978) Tyrosine free-radical in ribonucleotide reductase from *Escherichia coli*, *J. Biol. Chem. 253*, 6863−6865.
9. Sjöberg, B. M., Reichard, P., Gräslund, A., and Ehrenberg, A. (1977) Nature of free-radical in ribonucleotide reductase from *Escherichia coli*, *J. Biol. Chem. 252*, 536−541.
10. Mann, G. J., Gräslund, A., Ochiai, E. I., Ingemarson, R., and Thelander, L. (1991) Purification and characterization of recombinant mouse and herpes-simplex virus ribonucleotide reductase R2 subunit, *Biochemistry 30*, 1939−1947.
11. Guittet, O., Hakansson, P., Voevodskaya, N., Fridd, S., Gräslund, A., Arakawa, H., Nakamura, Y., and Thelander, L. (2001) Mammalian p53R2 protein forms an active ribonucleotide reductase *in vitro* with the R1 protein, which is expressed both in resting cells in response to DNA damage and in proliferating cells, *J. Biol. Chem. 276*, 40647−40651.
12. Hofer, A., Schmidt, P. P., Gräslund, A., and Thelander, L. (1997) Cloning and characterization of the R1 and R2 subunits of ribonucleotide reductase from *Trypanosoma brucei*, *Proc. Natl. Acad. Sci. U.S.A. 94*, 6959−6964.
13. Lamarche, N., Matton, G., Massie, B., Fontecave, M., Atta, M., Dumas, F., Gaudreau, P., and Langelier, Y. (1996) Production of the R2 subunit of ribonucleotide reductase from herpes simplex virus with prokaryotic and eukaryotic expression systems: Higher activity of R2 produced by eukaryotic cells related to higher iron-binding capacity, *Biochem. J. 320*, 129−135.
14. Perlstein, D. L., Ge, J., Ortigosa, A. D., Robblee, J. H., Zhang, Z., Huang, M., and Stubbe, J. (2005) The active form of the *S. cerevisiae* ribonucleotide reductase small subunit is a heterodimer *in vitro* and *in vivo*, *Biochemistry 44*, 15366−15377.
15. Chabes, A., Domkin, V., Larsson, G., Liu, A. M., Gräslund, A., Wijmenga, S., and Thelander, L. (2000) Yeast ribonucleotide reductase has a heterodimeric iron-radical-containing subunit, *Proc. Natl. Acad. Sci. U.S.A. 97*, 2474−2479.
16. Elleingand, E., Gerez, C., Un, S., Knupling, M., Lu, G., Salem, J., Rubin, H., Sauge-Merle, S., Laulhere, J. P., and Fontecave, M. (1998) Reactivity studies of the tyrosyl radical in ribonucleotide reductase from *Mycobacterium tuberculosis* and *Arabidopsis thaliana*: Comparison with *Escherichia coli* and mouse, *Eur. J. Biochem. 258*, 485−490.
17. Atkin, C. L., Thelander, L., Reichard, P., and Lang, G. (1973) Iron and free-radical in ribonucleotide reductase: Exchange of iron and Mössbauer spectroscopy of protein-B2 subunit of *Escherichia coli* enzyme, *J. Biol. Chem. 248*, 7464−7472.
18. Ehrenberg, A., and Reichard, P. (1972) Electron spin resonance of the iron-containing protein B2 from ribonucleotide reductase, *J. Biol. Chem. 247*, 3485−3488.
19. Fontecave, M., Eliasson, R., and Reichard, P. (1987) NAD(P)H-flavin oxidoreductase of *Escherichia coli*: A ferric iron reductase participating in the generation of the free-radical of ribonucleotide reductase, *J. Biol. Chem. 262*, 12325−12331.
20. Fontecave, M., Gräslund, A., and Reichard, P. (1987) The function of superoxide-dismutase during the enzymatic formation of the free-radical of ribonucleotide reductase, *J. Biol. Chem. 262*, 12332−12336.
21. Fontecave, M., and Reichard, P. (1987) A NAD(P)H-flavin oxidoreductase is involved in the activation of ribonucleotide reductase in *Escherichia coli*, *Recl. Trav. Chim. Pays-Bas 106*, 245.
22. Elledge, S. J., and Davis, R. W. (1990) Two genes differentially regulated in the cell-cycle and by DNA-damaging agents encode alternative regulatory subunits of ribonucleotide reductase, *Genes Dev. 4*, 740−751.
23. Domkin, V., Thelander, L., and Chabes, A. (2002) Yeast DNA damage-inducible Rnr3 has a very low catalytic activity strongly stimulated after the formation of a cross-talking Rnr1/Rnr3 complex, *J. Biol. Chem. 277*, 18574−18578.
24. Elledge, S. J., Zheng, Z., and Allen, J. B. (1992) Ribonucleotide reductase: Regulation, regulation, regulation, *Trends Biochem. Sci. 17*, 119−123.
25. Elledge, S. J., and Davis, R. W. (1987) Identification and isolation of the gene encoding the small subunit of ribonucleotide reductase from *Saccharomyces cerevisiae*: DNA damage-inducible gene required for mitotic viability, *Mol. Cell. Biol. 7*, 2783−2793.
26. Huang, M. X., and Elledge, S. J. (1997) Identification of RNR4, encoding a second essential small subunit of ribonucleotide reductase in *Saccharomyces cerevisiae*, *Mol. Cell. Biol. 17*, 6105−6113.
27. Wang, P. J., Chabes, A., Casagrande, R., Tian, X. C., Thelander, L., and Huffaker, T. C. (1997) Rnr4p, a novel ribonucleotide reductase small-subunit protein, *Mol. Cell. Biol. 17*, 6114−6121.
28. Ge, H., Perlstein, D. L., Nguyen, H. H., Bar, G., Griffin, R. G., and Stubbe, J. (2001) Why multiple small subunits (Y2 and Y4) for yeast ribonucleotide reductase? Toward understanding the role of Y4, *Proc. Natl. Acad. Sci. U.S.A. 98*, 10067−10072.
29. Voegtli, W. C., Ge, J., Perlstein, D. L., Stubbe, J., and Rosenzweig, A. C. (2001) Structure of the yeast ribonucleotide reductase Y2Y4 heterodimer, *Proc. Natl. Acad. Sci. U.S.A. 98*, 10073−10078.
30. Nguyen, H. H. T., Ge, J., Perlstein, D. L., and Stubbe, J. (1999) Purification of ribonucleotide reductase subunits Y1, Y2, Y3, and Y4 from yeast: Y4 plays a key role in di-iron cluster assembly, *Proc. Natl. Acad. Sci. U.S.A. 96*, 12339−12344.
31. Huang, M. X., Zhou, Z., and Elledge, S. J. (1998) The DNA replication and damage checkpoint pathways induce transcription by inhibition of the Crt1 repressor, *Cell 94*, 595−605.
32. Zaim, J., Speina, E., and Kierzek, A. M. (2005) Identification of new genes regulated by the Crt1 transcription factor, an effector of the DNA damage checkpoint pathway in *Saccharomyces cerevisiae*, *J. Biol. Chem. 280*, 28−37.
33. Gasch, A. P., Huang, M. X., Metzner, S., Botstein, D., Elledge, S. J., and Brown, P. O. (2001) Genomic expression responses to DNA-damaging agents and the regulatory role of the yeast ATR homolog Mec1p, *Mol. Biol. Cell 12*, 2987−3003.
34. Stookey, L. L. (1970) Ferrozine: A new spectrophotometric reagent for iron, *Anal. Chem. 42*, 779−782.
35. Winzeler, E. A., Shoemaker, D. D., Astromoff, A., Liang, H., Anderson, K., Andre, B., Bangham, R., Benito, R., Boeke, J. D., Bussey, H., Chu, A. M., Connelly, C., Davis, K., Dietrich, F., Dow, S. W., El Bakkoury, M., Foury, F., Friend, S. H., Gentalen, E., Giaever, G., Hegemann, J. H., Jones, T., Laub, M., Liao, H., Liebundguth, N., Lockhart, D. J., Lucau-Danila, A., Lussier, M., M'Rabet, N., Menard, P., Mittmann, M., Pai, C., Rebischung, C., Revuelta, J. L., Riles, L., Roberts, C. J., Ross-MacDonald, P., Scherens, B., Snyder, M., Sookhai-Mahadeo, S., Storms, R. K., Veronneau, S., Voet, M., Volckaert, G., Ward, T. R., Wysocki, R., Yen, G. S., Yu, K. X., Zimmermann, K., Philippsen, P., Johnston, M., and Davis, R. W. (1999) Functional characterization of the *S. cerevisiae* genome by gene deletion and parallel analysis, *Science 285*, 901−906.
36. Lunn, C. A., Kathju, S., Wallace, B. J., Kushner, S. R., and Pigiet, V. (1984) Amplification and purification of plasmid-encoded thioredoxin from *Escherichia coli* K12, *J. Biol. Chem. 259*, 10469−10474.
37. Russel, M., and Model, P. (1985) Direct cloning of the Trxb gene that encodes thioredoxin reductase, *J. Bacteriol. 163*, 238−242.
38. Steeper, J. R., and Steuart, C. D. (1970) A rapid assay for CDP reductase activity in mammalian cell extracts, *Anal. Biochem. 34*, 123−130.
39. Bollinger, J. M., Tong, W. H., Ravi, N., Huynh, B. H., Edmondson, D. E., and Stubbe, J. (1995) Use of rapid kinetics methods to study the assembly of the diferric-tyrosyl radical cofactor of *Escherichia coli* ribonucleotide reductase, *Methods Enzymol. 258*, 278−303.
40. Malmstrom, B. G., Reinhammar, B., and Vanngard, T. (1970) The state of copper in stellacyanin and laccase from the lacquer tree *Rhus vernicifera*, *Biochim. Biophys. Acta 205*, 48−57.
41. Jorgensen, P., Nishikawa, J. L., Breitkreutz, B. J., and Tyers, M. (2002) Systematic identification of pathways that couple cell growth and division in yeast, *Science 297*, 395−400.
42. Sherman, F. (1991) Getting started with yeast, *Methods Enzymol. 194*, 3−21.
43. Climent, I., Sjöberg, B. M., and Huang, C. Y. (1992) Site-directed mutagenesis and deletion of the carboxyl terminus of *Escherichia coli* ribonucleotide reductase protein R2: Effects on catalytic activity and subunit interaction, *Biochemistry 31*, 4801−4807.
44. Fisher, A., Yang, F. D., Rubin, H., and Cooperman, B. S. (1993) R2 C-terminal peptide inhibition of mammalian and yeast ribonucleotide reductase, *J. Med. Chem. 36*, 3859−3862.

45. Kasrayan, A., Birgander, P. L., Pappalardo, L., Regnstrom, K., Westman, M., Slaby, A., Gordon, E., and Sjöberg, B. M. (2004) Enhancement by effectors and substrate nucleotides of R1-R2 interactions in *Escherichia coli* class Ia ribonucleotide reductase, *J. Biol. Chem. 279*, 31050−31057.
46. Yao, R. J., Zhang, Z., An, X. X., Bucci, B., Perlstein, D. L., Stubbe, J., and Huang, M. X. (2003) Subcellular localization of yeast ribonucleotide reductase regulated by the DNA replication and damage checkpoint pathways, *Proc. Natl. Acad. Sci. U.S.A. 100*, 6628−6633.
47. Thelander, L. (1973) Physiochemical characterization of ribonucleoside diphosphate reductase from *Escherichia coli*, *J. Biol. Chem. 248*, 4591−4601.
48. Ochiai, E. I., Mann, G. J., Gräslund, A., and Thelander, L. (1990) Tyrosyl free-radical formation in the small subunit of mouse ribonucleotide reductase, *J. Biol. Chem. 265*, 15758−15761.
49. Howell, M. L., Sandersloehr, J., Loehr, T. M., Roseman, N. A., Mathews, C. K., and Slabaugh, M. B. (1992) Cloning of the vaccinia virus ribonucleotide reductase small subunit gene: Characterization of the gene-product expressed in *Escherichia coli*, *J. Biol. Chem. 267*, 1705−1711.
50. SaugeMerle, S., Laulhere, J. P., Coves, J., LePape, L., Menage, S., and Fontecave, M. (1997) Ribonucleotide reductase from the higher plant *Arabidopsis thaliana*: Expression of the R2 component and characterization of its iron-radical center, *J. Biol. Inorg. Chem. 2*, 586−594.
51. Fontecave, M., Eliasson, R., and Reichard, P. (1989) Enzymatic regulation of the radical content of the small subunit of *Escherichia coli* ribonucleotide reductase involving reduction of its redox centers, *J. Biol. Chem. 264*, 9164−9170.
52. Eliasson, R., Jornvall, H., and Reichard, P. (1986) Superoxide-dismutase participates in the enzymatic formation of the tyrosine radical of ribonucleotide reductase from *Escherichia coli*, *Proc. Natl. Acad. Sci. U.S.A. 83*, 2373−2377.
53. Coves, J., Niviere, V., Eschenbrenner, M., and Fontecave, M. (1993) NADPH-sulfite reductase from *Escherichia coli*: A flavin reductase participating in the generation of the free-radical of ribonucleotide reductase, *J. Biol. Chem. 268*, 18604−18609.
54. McCarroll, R. M., and Fangman, W. L. (1988) Time of replication of yeast centromeres and telomeres, *Cell 54*, 505−513.
55. Stubbe, J., and Riggs-Gelasco, P. (1998) Harnessing free radicals: Formation and function of the tyrosyl radical in ribonucleotide reductase, *Trends Biochem. Sci. 23*, 438−443.
56. Harder, J., and Follmann, H. (1990) Identification of a free-radical and oxygen dependence of ribonucleotide reductase in yeast, *Free Radical Res. Commun. 10*, 281−286.
57. Ge, J., Yu, G. X., Ator, M. A., and Stubbe, J. (2003) Pre-steady-state and steady-state kinetic analysis of *E. coli* class I ribonucleotide reductase, *Biochemistry 42*, 10071−10083.
58. Qiu, W., Zhou, B., Darwish, D., Shao, J., and Yen, Y. (2006) Characterization of enzymatic properties of human ribonucleotide reductase holoenzyme reconstituted *in vitro* from hRRM1, hRRM2 and p53R2 subunits, *Biochem. Biophys. Res. Commun. 340*, 428−434.
59. Desany, B. A., Alcasabas, A. A., Bachant, J. B., and Elledge, S. J. (1998) Recovery from DNA replicational stress is the essential function of the S-phase checkpoint pathway, *Genes Dev. 12*, 2956−2970.
60. Chabes, A., Georgieva, B., Domkin, V., Zhao, X. L., Rothstein, R., and Thelander, L. (2003) Survival of DNA damage in yeast directly depends on increased dNTP levels allowed by relaxed feedback inhibition of ribonucleotide reductase, *Cell 112*, 391−401.
61. Weinberg, G., Ullman, B., and Martin, D. W. (1981) Mutator phenotypes in mammalian-cell mutants with distinct biochemical defects and abnormal deoxyribonucleoside triphosphate pools, *Proc. Natl. Acad. Sci. U.S.A. 78*, 2447−2451.
62. Reichard, P. (1988) Interactions between deoxyribonucleotide and DNA synthesis, *Annu. Rev. Biochem. 57*, 349−374.
63. Thelander, L., and Reichard, P. (1979) Reduction of ribonucleotides, *Annu. Rev. Biochem. 48*, 133−158.
64. Larsson, K. M., Jordan, A., Eliasson, R., Reichard, P., Logan, D. T., and Nordlund, P. (2004) Structural mechanism of allosteric substrate specificity regulation in a ribonucleotide reductase, *Nat. Struct. Mol. Biol. 11*, 1142−1149.
65. Björklund, S., Skog, S., Tribukait, B., and Thelander, L. (1990) S-Phase-specific expression of mammalian ribonucleotide reductase R1 and reductase R2 subunit messenger RNAs, *Biochemistry 29*, 5452−5458.
66. Koch, C., Moll, T., Neuberg, M., Ahorn, H., and Nasmyth, K. (1993) A role for the transcription factors Mbp1 and Swi4 in progression from G1 to S-phase, *Science 261*, 1551−1557.
67. Liu, X., Zhou, B., Xue, L., Shih, J., Tye, K., Qi, C., and Yen, Y. (2005) The ribonucleotide reductase subunit M2B subcellular localization and functional importance for DNA replication in physiological growth of KB cells, *Biochem. Pharmacol.* (in press).
68. Lincker, F., Philipps, G., and Chaboute, M. E. (2004) UV-C response of the ribonucleotide reductase large subunit involves both E2F-mediated gene transcriptional regulation and protein subcellular relocalization in tobacco cells, *Nucleic Acids Res. 32*, 1430−1438.
69. Chabes, A., and Thelander, L. (2000) Controlled protein degradation regulates ribonucleotide reductase activity in proliferating mammalian cells during the normal cell cycle and in response to DNA damage and replication blocks, *J. Biol. Chem. 275*, 17747−17753.
70. Zhao, X. L., and Rothstein, R. (2002) The Dun1 checkpoint kinase phosphorylates and regulates the ribonucleotide reductase inhibitor Sml1, *Proc. Natl. Acad. Sci. U.S.A. 99*, 3746−3751.
71. Standart, N., Hunt, T., and Ruderman, J. V. (1986) Differential accumulation of ribonucleotide reductase subunits in clam oocytes: The large subunit is stored as a polypeptide, the small subunit as untranslated messenger-RNA, *J. Cell Biol. 103*, 2129−2136.
72. Koc, A., Wheeler, L. J., Mathews, C. K., and Merrill, G. F. (2003) Replication-independent Mcb gene induction and deoxyribonucleotide accumulation at G_1/S in *Saccharomyces cerevisiae*, *J. Biol. Chem. 278*, 9345−9352.
73. Petersson, L., Gräslund, A., Ehrenberg, A., Sjöberg, B. M., and Reichard, P. (1980) The iron center in ribonucleotide reductase from *Escherichia coli*, *J. Biol. Chem. 255*, 6706−6712.
74. Chabes, A., Domkin, V., and Thelander, L. (1999) Yeast Sml1, a protein inhibitor of ribonucleotide reductase, *J. Biol. Chem. 274*, 36679−36683.
75. Davis, R., Thelander, M., Mann, G. J., Behravan, G., Soucy, F., Beaulieu, P., Lavallee, P., Gräslund, A., and Thelander, L. (1994) Purification, characterization, and localization of subunit interaction area of recombinant mouse ribonucleotide reductase R1 subunit, *J. Biol. Chem. 269*, 23171−23176.
76. Koc, A., Matthews, C. K., Wheeler, L. J., Gross, M. K., and Merrill, G. F. (2006) Thioredoxin is required for deoxyribonucleotide pool maintenance during S phase, *J. Biol. Chem.* (in press).
77. Shao, J. M., Zhou, B. S., Zhu, L. J., Qiu, W. H., Yuan, Y. C., Xi, B. X., and Yen, Y. (2004) In vitro characterization of enzymatic properties and inhibition of the p53R2 subunit of human ribonucleotide reductase, *Cancer Res. 64*, 1−6.
78. Zhao, X. L., Georgieva, B., Chabes, A., Domkin, V., Ippel, J. H., Schleucher, J., Wijmenga, S., Thelander, L., and Rothstein, R. (2000) Mutational and structural analyses of the ribonucleotide reductase inhibitor Sml1 define its Rnr1 interaction domain whose inactivation allows suppression of Mec1 and Rad53 lethality, *Mol. Cell. Biol. 20*, 9076−9083.
79. Uchiki, T., Dice, L. T., Hettich, R. L., and Dealwis, C. (2004) Identification of phosphorylation sites on the yeast ribonucleotide reductase inhibitor Sml1, *J. Biol. Chem. 279*, 11293−11303.

BI0610404